Polymer 52 (2011) 2189–2197

Contents lists available at ScienceDirect

Polymer

journal homepage: www.elsevier.com/locate/polymer

Synthesis and characterization of red light-emitting electrophosphorescent polymers with different triplet energy main chain

Zhihua Ma [a,b,1], Junqiao Ding [a,*], Yanxiang Cheng [a], Zhiyuan Xie [a], Lixiang Wang [a,*], Xiabin Jing [a], Fosong Wang [a]

[a] State Key Laboratory of Polymer Physics and Chemistry, Changchun Institute of Applied Chemistry, Chinese Academy of Sciences, Changchun 130022, PR China
[b] Graduate School of the Chinese Academy of Sciences, Beijing 100039, PR China

ARTICLE INFO

Article history:
Received 19 January 2011
Received in revised form
6 March 2011
Accepted 15 March 2011
Available online 21 March 2011

Keywords:
Electrophosphorescent polymers
Light emitting diodes
Triplet energy

ABSTRACT

Red light-emitting electrophosphorescent polymers with poly(fluorene-*alt*-carbazole) (PFCz) and poly (3,6-carbazole) (PCz) as the main chain, and the quinoline-based iridium (Ir) complex as the side chain have been synthesized by Suzuki and modified Yamamoto polymerization, respectively. The triplet energy of the polymeric backbone is tuned from 2.1 eV of polyfluorene (PF) to 2.3 eV of PFCz and 2.6 eV of PCz. We find that, with the increasing triplet energy, the lifetime of the triplet excitons gradually increases, but the device efficiency becomes worse. The reason is that the alteration of the main chain structure leads to the increase of the highest occupied molecular orbital (HOMO) level of the polymeric host, which can facilitate the efficient hole injection and transportation. As a consequence of this enhancement of the hole current, charge balance in the emitting layer is destroyed, and correspondingly, the poorer device performance is achieved. Our results, we believe, indicate that besides the triplet energy, charge balance is a crucial determinant to develop high efficiency red light-emitting electrophosphorescent polymers.

1. Introduction

Electrophosphorescent polymeric light-emitting devices (PhPLEDs) have drawn great attention due to their ability to integrate the low-cost solution processability of the polymers [1] and the high efficiency of the electrophosphorescent transition metal complexes [2]. Up to now, there are generally two strategies to realize PhPLEDs. One is physical blending the phosphor with the polymer host. However, these devices bear some problems, such as potential aggregation and phase separation, which can result in triplet–triplet annihilation, and thus lead to the fast decay of the device efficiency at high current density [3–6].

Therefore, the other way, chemical attaching the phosphor to the polymer host, has been developed. In early 2003, Chen and coworkers reported electrophosphorescent polymers based on polyfluorene (PF) backbone with bis[2-(2′-benzothienyl) pridinato-N,$C^{3'}$](acetylacetonato) Ir complex [$(btp)_2$Ir(acac)] as the pendant attached to the 9-carbon position of fluorene. When carbazole was introduced as the side chain, the device showed a luminous efficiency of 2.8 cd/A at 7.0 V and a luminance of 65 cd/m^2 with the peak emission at 610 nm [7]. By introducing isoquinoline-based Ir complex as the side chain of poly(fluorene-*alt*-carbazole) (PFCz) copolymers, Jiang et al. further improved the efficiency to 4.0 cd/A [8]. Recently, we have realized an unexpected high efficiency based on a simple polymeric chain owing to the charge balance. When 1 mol % of the quinoline-based Ir complex was incorporated into the side chain of PF, a high efficiency of 5.0 cd/A was achieved for the single layer device. Additionally, by inserting an alcohol-soluble electron injection layer, the luminous efficiency was optimized to 8.3 cd/A [9].

Nonetheless, we note that the triplet energy (E_T) of PF (2.1 eV) is nearly the same as that of the quinoline-based Ir complex (2.1 eV) [10]. It remains unknown whether the back energy transfer from the dopant to PF happens in this system, and to what extent it affects the device performance [11]. To clarify this doubt, in this article, we change the main chain from PF to PFCz and poly(3,6-carbazole) (PCz), which have higher E_T levels (PFCz: 2.3 eV; PCz: 2.6 eV) than that of PF, and synthesize two series of the corresponding red light-emitting phosphorescent polymers, PFCz05R0–PFCz5R0 and PCz05R0–PCz5R0. In comparison to polymer PF1R0, the lifetimes of PFCz1R0 and PCz1R0 gradually increase with the increasing E_T of the

* Corresponding authors.
E-mail addresses: junqiaod@ciac.jl.cn (J. Ding), lixiang@ciac.jl.cn (L. Wang).
[1] Fax: +86 0431 8568 5653.

0032-3861/$ – see front matter © 2011 Elsevier Ltd. All rights reserved.
doi:10.1016/j.polymer.2011.03.023

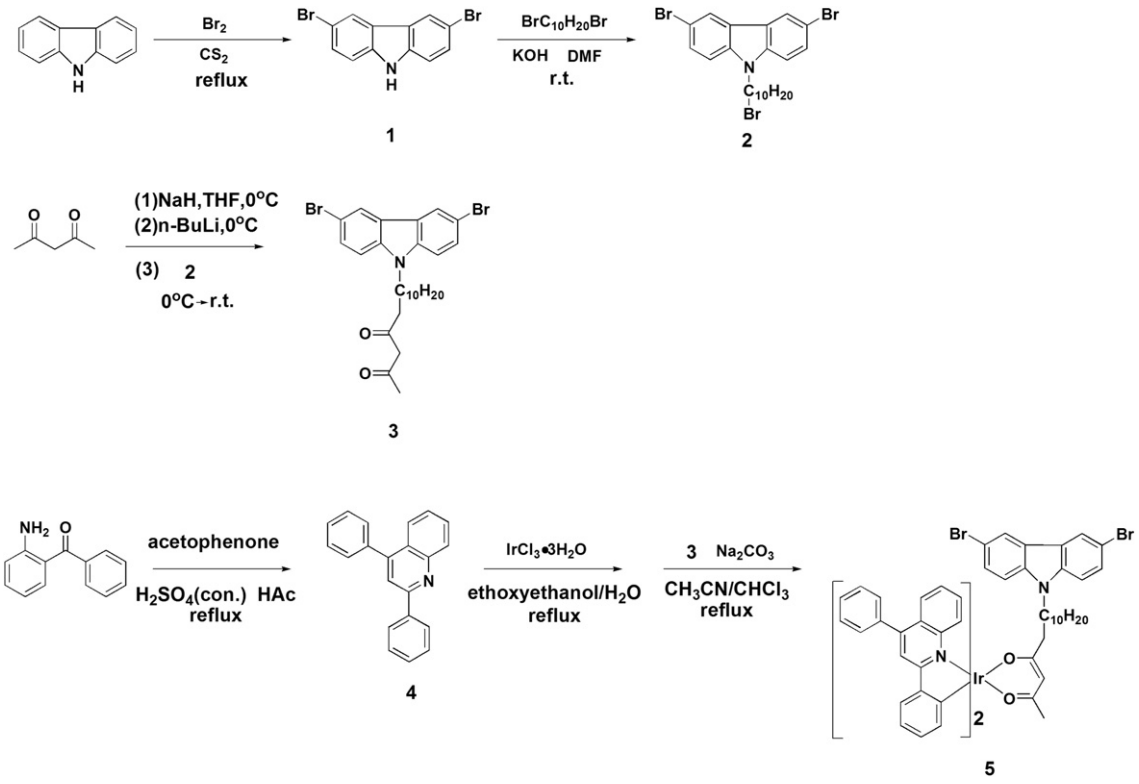

Scheme 1. Synthetic route of the complex monomer.

main chain, indicative of the efficient confinement of the triplet excitons on the phosphors. Notably, accompanied by the alteration of the backbone's structure, we find that the highest occupied molecular orbital (HOMO) levels of the polymeric hosts have increased to facilitate the hole injection as well as the transportation due to the reduced hole injection barrier and hole-trap depth. As a result, the balance between holes and electrons in the emitting layer is disrupted, and thus the device performance decreases from 5.0 cd/A of PF1R0 to 1.7 cd/A of PFCz1R0 and 0.3 cd/A of PCz1R0, respectively. Our results suggest that apart from the triplet energy of the polymeric host, charge balance is a crucial determinant of high efficiency PhPLEDs.

2. Experimental

2.1. Materials and characterization

All reagents were purchased from Aldrich or Acros and used without further purification. THF, DMF and toluene were purified according to standard procedures. 2,4-diphenyl-quinoline (**4**) (PPQ) [12], 3,6-dibromo-N-decylcarbazole (**6**) [13] and 2,7-bis-(trimethyleneborate)-9,9-dioctylfluorene (**7**) [7] were prepared according to the literature procedure. ^{1}H NMR spectra were obtained with a Bruker Avance 300NMR spectrometer. The chemical shifts with respect to tetramethylsilane as an internal reference are reported in parts per million. Fourier transform infrared (FTIR) spectra were recorded on a Bruker Vertex 70 spectrometer with KBr pellets. Elemental analysis was performed using a Bio-Rad elemental analysis system. Number- and weight-average molecular weights (M_n and M_w) together with the polydispersity indexes of the polymers were determined by gel permeation chromatography (GPC) on a Waters 410 instrument with polystyrene as a standard and THF as the eluent. Thermal properties of the polymers were analyzed with a Perkin–Elmer-TGA 7 instrument under nitrogen at a heating rate of 10 °C min^{-1}. UV–Vis absorption spectra were recorded by a Perkin–Elmer Lambda 35 UV–Vis spectrometer. PL spectra were recorded using a Perkin–Elmer LS50B spectrofluorometer. The PL decay curves were obtained from a Lecroy Wave Runner 6100 digital oscilloscope (1 GHz) by using a tunable laser (pulse width = 4 ns, gate = 50 ns) as excitation source (Continuum Sunlite OPO).

2.2. Synthesis

2.2.1. 3,6-Dibromocarbazole (1)

6.8 mL bromine (21.1 g, 132 mmol) dissolved in 30 mL carbon disulfide was added dropwise to a suspension of carbazole (10.0 g, 60 mmol) in 120 mL carbon disulfide at 50 °C. After the addition, the reaction was further stirred for 5 h. Then the reaction was cooled to room temperature, the solid was filtered and washed with carbon disulfide twice. The final product was recrystallized from ethanol (9.2 g, 47.0%). ^{1}H NMR (300 MHz, $CDCl_3$): δ 8.13 (d, J = 1.8 Hz, 2H), 8.08 (br, 1H), 7.52 (dd, J = 8.7 Hz, 2H), 7.31 (d, J = 8.7 Hz, 2H).

2.2.2. 3,6-Dibromo-N-(10-bromodecyl)-carbazole (2)

To a stirred suspension of 3,6-dibromocarbazole **1** (3.0 g, 9.2 mmol) and KOH (0.9 g, 15.5 mmol) in 50 mL DMF, 1,10-dibromodecane (6.3 mL, 27.7 mmol) was added at room temperature. After 24 h, the reaction mixture was poured into water, and extracted with DCM (100 mL ×3), then the combined organic phase was washed with water for 3 times and dried over anhydrous sodium sulfate. After removal of the solvent, the excess of 1,10-dibromodecane was recovered from the mixture at 120 °C under reduced pressure. The crude product was purified by silica gel column with petroleum: DCM = 10:1 as eluent to give white solid

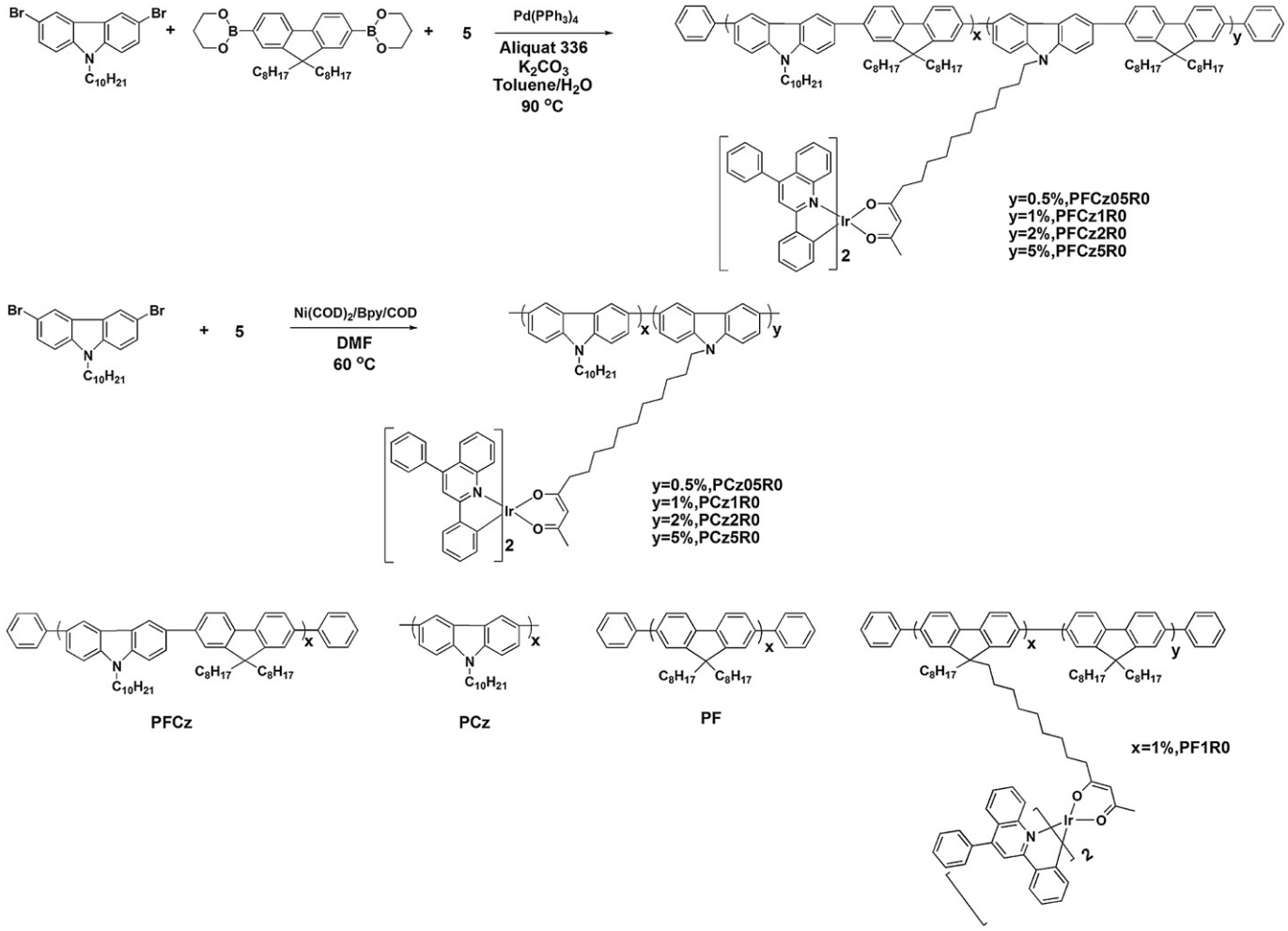

Scheme 2. Synthetic routes of the polymers and the molecular structures of PFCz, PCz, PF as well as PF1R0.

(3.0 g, 58.8%). ^{1}H NMR (300 MHz, $CDCl_3$): δ 8.13 (d, J = 1.8 Hz, 2H), 7.54 (dd, J = 8.7 Hz, 2H), 7.25 (d, J = 8.7 Hz, 2H), 4.22 (t, J = 7.2 Hz, 2H), 3.39 (t, J = 6.6 Hz, 2H), 1.87–1.77 (m, 4H), 1.40–1.23 (m, 12H).

2.2.3. *N-(12,14-dioxo-quindecyl)-3,6-dibromocarbazole (3) [14]*

Sodium hydride (50 wt% in mineral oil; 2.1 g, 42.5 mmol) was washed with THF (20 mL each) three times. Acetylacetone (4.0 mL, 36.4 mmol) was added dropwise to a stirred suspension of sodium hydride in THF (80 mL) at 0 °C. The resultant mixture was stirred for a further 30 min at 0 °C. N-butyllithium (1.6 M in hexane; 22.8 mL, 36.4 mmol) was added dropwise to the mixture at 0 °C and the resultant mixture was stirred for a further 30 min at 0 °C. 3,6-Dibromo-N-(10-bromodecyl)-carbazole **2** (6.6 g, 12.2 mmol) dissolved in THF (25 mL) was added to the stirred solution dropwisely at 0 °C. The reaction was kept at 0 °C for 1 h and a further 1 h at room temperature, after which it was quenched with aqueous ammonium chloride (10 wt%, 40 mL). Concentrated hydrochloric acid was added to the mixture until pH 1 was reached, and then the

Table 1
Molecular Weights and Thermal Properties of Polymers.

Polymer	M_n[a]	M_w[a]	PDI[a]	T_g[b] (°C)	T_d[c] (°C)	(**6** + **7**) or **6**/**BrCzR0** (molar ratio)[d]	
						monomer in feed ratio	composition in polymer[e]
PFCz05R0	18,000	40,000	2.21	101	418	99.5/0.5	–
PFCz1R0	17,000	36,000	2.14	102	416	99/1	–
PFCz2R0	19,000	39,000	2.54	105	418	98/2	99.4/0.6
PFCz5R0	20,000	52,000	2.56	106	358	95/5	96.9/3.1
PCz05R0	32,000	48,000	1.51	128	437	99.5/0.5	–
PCz1R0	45,000	89,000	1.95	128	443	99/1	–
PCz2R0	64,000	129,000	2.01	135	441	98/2	99.7/0.3
PCz5R0	78,000	168,000	2.16	137	350	95/5	98.6/1.4

[a] Determined by GPC using THF as eluent with polystyrene as the standard.
[b] Glass transition temperature measured by DSC under nitrogen at a heating rate of 10 °C/min.
[c] Temperature of 5% weight loss measured by TGA in nitrogen.
[d] For PFCz-based polymers, the molar ratio is (**6** + **7**)/**BrCzR0**; For PCz-based polymers, the molar ratio is **6**/**BrCzR0**.
[e] Calculated according to ^{1}H NMR spectra.

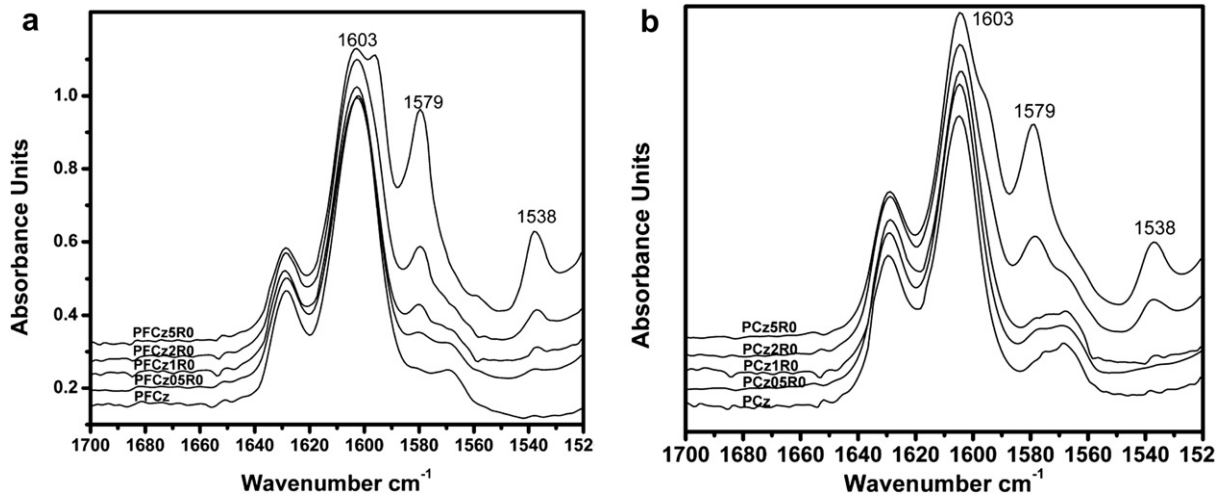

Fig. 1. IR spectra of the polymers. (a) PFCz-based polymers and PFCz; (b) PCz-based polymers and PCz.

aqueous phase was separated and extracted with diethyl ether. The combined organic phases were washed with saturated sodium bicarbonate, dried over anhydrous sodium sulfate. After removal of the solvent, the crude product was purified by silica gel column with petroleum: DCM = 2:1 as eluent to give a white solid (4.8 g, 70.8%). ^{1}H NMR (300 MHz, $CDCl_3$): δ 15.48 (br, 0.8H), 8.13 (d, J = 1.8 Hz, 2H), 7.54 (dd, J = 8.6 Hz, 2H), 7.26 (d, J = 8.7 Hz, 2H), 5.48 (s, 0.8H), 4.23 (t, J = 7.2 Hz, 2H), 3.56 (s, 0.4H), 2.48 (t, J = 7.5 Hz, 0.4H), 2.25 (t, J = 7.2 Hz, 1.6H), 2.23 (s, 0.4H), 2.05 (s, 1.6H), 1.88–1.77 (m, 2H), 1.62–1.53 (m, 2H), 1.28–1.21 (m, 14H).

2.2.4. 9-(iridium(III)bis(2,4-diphenyl-quinoline-N,C$^{2'}$) (quindecanedionate-12,14))-3,6-dibromocarbazole (5)

Cyclometalated Ir(III) μ-chloro-bridged dimer was synthesized according to the Nonoyama method [15]. Iridium chloride trihydrate (0.88 g, 2.5 mmol) and 2,4-diphenyl-quinoline **4** (1.48 g, 5.3 mmol) were added to a mixed solvent of ethoxyethanol (45 mL) and water (15 mL). The mixture was refluxed for 24 h. After cooling to room temperature, the precipitate was collected by filtration and purified by alkaline alumina column with petroleum: DCM = 2:1 to DCM: methanol = 50:1 as eluent. The resulting dimer (0.77 g, 0.56 mmol), N-(12,14-dioxo-quindecyl)-3,6-dibromocarbazole **3** (0.64 g, 1.15 mmol) and sodium carbonate (0.60 g, 5.6 mmol) were added to a mixed solvent of acetonitrile (15 mL) and chloroform (15 mL). The mixture was refluxed for 24 h before cooling to room temperature. Then the resultant mixture was poured into water and extracted with DCM. The organic phase was washed with brine and dried with anhydrous sodium sulfate. After removal of the solvent, the crude product was purified by alkaline alumina column with petroleum: DCM = 2:1 as eluent to give a red solid (0.33 g, 22.4%). ^{1}H NMR (300 MHz, $CDCl_3$): δ 8.59–8.52 (m, 2H), 8.15 (s, 2H), 8.03 (s, 1H), 7.97 (s, 1H), 7.87–7.78 (m, 4H), 7.70–7.50 (m, 12H), 7.73–7.40 (m, 4H), 7.26 (d, J = 14.1 Hz, 2H), 6.96–6.88 (m, 2H), 6.70–6.55 (m, 4H), 4.68 (s, 1H), 4.23 (t, J = 6.9 Hz, 2H), 1.83–1.64 (m, 4H), 1.53–1.54 (m, 4H), 1.26–0.80 (m, 15H). IR (KBr, cm^{-1}): 3055 (w), 2922 (s), 2850 (s), 1594 (s), 1578 (s), 1536 (s), 1513 (s), 1494 (s), 1445 (s), 1406 (s), 1379 (s), 1288 (s), 1264 (s), 1047 (s), 762 (s), 701 (s).

2.2.5. General procedure of the Suzuki polymerization

To a mixture of 3,6-dibromo-N-decylcarbazole **6**, 2,7-bis-(trimethyleneborate)-9,9-dioctylfluorene **7** and 9-(iridium(III)bis(2,4-diphenyl-quinoline-N,C$^{2'}$)(quindecanedionate-12,14))-3,6-dibromocarbazole **5** with the corresponding feed ratios, aliquat 336 (20 mg) and $Pd(PPh_3)_4$ (1 mol %) were added. The mixture was degassed for 30 min, and then 2 M degassed aqueous K_2CO_3 (3 mL) and degassed toluene (8 mL) were added under argon. The mixture was heated to 90 °C and stirred for 24 h in the dark. Then the end-capping reagents were added. First phenylboronic acid (100 mg) stirring for 12 h, and then bromobenzene (0.5 mL) for another 12 h. After workup, the mixture was poured into methanol. The precipitate

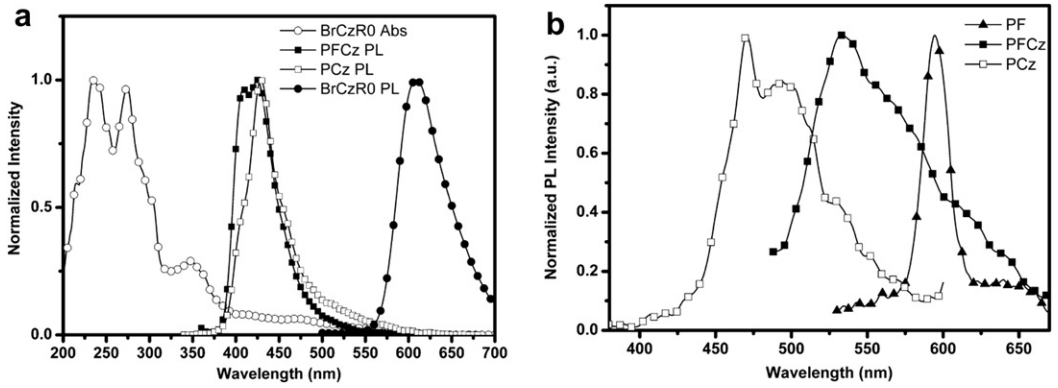

Fig. 2. The absorption spectrum in DCM and PL spectrum in toluene of BrCzR0 as well as the PL spectra of PFCz and PCz in films (a) and the phosphorescent spectra of PF, PFCz and PCz (b).

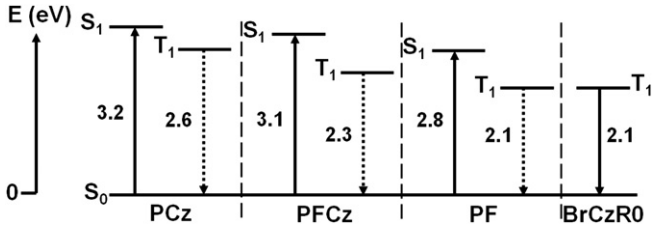

Fig. 3. Energy level diagram containing the singlet ground state (S_0), the lowest excited singlet state (S_1), and the lowest excited triplet state (T_1) of the polymer hosts, as well as the T_1 level of the complex monomer BrCzR0.

was collected by filtration and then dissolved in DCM. The solution was then washed with water and then dried with anhydrous sodium sulfate. The solution was concentrated to an appropriate volume and then poured into methanol to get polymer fibers. The polymer was purified by Soxhlet extraction in acetone for 48 h. The reprecipitation procedure in DCM/methanol was then repeated for several times. The final product was obtained after drying in vacuum with a yield of 50%–60%.

2.2.5.1. PFCz05R0. 3,6-dibromo-N-decylcarbazole **6** (230.3 mg, 0.495 mmol), **BrCzR0** (6.6 mg, 0.005 mmol), 2,7-bis-(trimethyleneborate)-9,9-dioctylfluorene **7** (279.2 mg, 0.5 mmol) were used in the polymerization. ^{1}H NMR (300 MHz, $CDCl_3$): δ 8.50 (s, 2H), 7.85 (d, J = 7.5 Hz, 4H), 7.77–7.73 (m, 4H), 7.53 (d, J = 8.4 Hz, 2H), 4.39 (s, 2H), 2.14 (br, 4H), 1.96 (br, 2H), 1.26–1.11 (m, 38H), 0.89–0.74 (m, 9H). Anal Calcd for $(C_{29}H_{40})_{50}(C_{22}H_{27}N)_{49.5}(C_{69}H_{61}IrN_3O_2)_{0.5}$: C, 87.99; H, 9.66; N, 2.03. Found: C, 86.65; H, 9.76; N, 1.68. IR (KBr, cm^{-1}): 2954 (s), 2926 (s), 2854 (s), 1862 (w), 1628 (w), 1603 (m), 1496 (s), 1463 (s), 1378 (m), 1268 (m), 879 (m), 825 (m), 802 (s), 757 (w), 722 (w).

2.2.5.2. PFCz1R0. 3,6-dibromo-N-decylcarbazole **6** (228.0 mg, 0.49 mmol), **BrCzR0** (13.2 mg, 0.01 mmol), 2,7-bis-(trimethyleneborate)-9,9-dioctylfluorene **7** (279.2 mg, 0.5 mmol) were used in the polymerization. ^{1}H NMR (300 MHz, $CDCl_3$): δ 8.50 (s, 2H), 7.84 (d, J = 7.5 Hz, 4H), 7.77–7.73 (m, 4H), 7.53 (d, J = 8.4 Hz, 2H), 4.39 (s, 2H), 2.14 (br, 4H), 1.96 (br, 2H), 1.26–1.11 (m, 38H), 0.89–0.74 (m, 9H). Anal Calcd for $(C_{29}H_{40})_{50}(C_{22}H_{27}N)_{49}(C_{69}H_{61}IrN_3O_2)_1$: C, 87.73; H, 9.59; N, 2.05. Found: C, 87.26; H, 9.24; N, 2.36. IR (KBr, cm^{-1}): 2954 (s), 2926 (s), 2854 (s), 1862 (w), 1629 (w), 1603 (m), 1496 (m), 1463 (s), 1378 (m), 1268 (m), 879 (m), 825 (m), 802 (s), 757 (w), 722 (w).

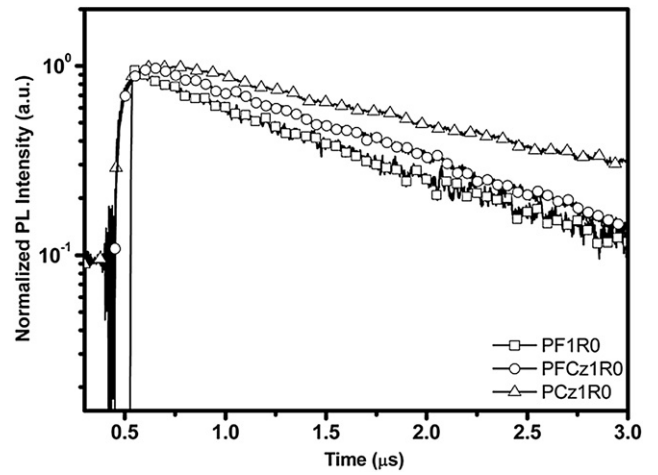

Fig. 4. Decay of the PL intensity (excited at 355 nm) at room temperature from thin films of PF1R0, PFCz1R0, PCz1R0.

2.2.5.3. PFCz2R0. 3,6-dibromo-N-decylcarbazole **6** (223.3 mg, 0.48 mmol), **BrCzR0** (26.3 mg, 0.02 mmol), 2,7-bis-(trimethyleneborate)-9,9-dioctylfluorene **7** (279.2 mg, 0.5 mmol) were used in the polymerization. ^{1}H NMR (300 MHz, $CDCl_3$): δ 8.50 (s, 2H), 7.85 (d, J = 7.5 Hz, 4H), 7.77–7.73 (m, 4H), 7.53 (d, J = 8.4 Hz, 2H), 6.96–6.90 (m, ArH of Ir(PPQ)), 6.65–6.58 (m, ArH of Ir(PPQ)), 4.39 (s, 2H), 2.14 (br, 4H), 1.96 (br, 2H), 1.26–1.11 (m, 38H), 0.89–0.74 (m, 9H). Anal Calcd for $(C_{29}H_{40})_{50}(C_{22}H_{27}N)_{48}(C_{69}H_{61}IrN_3O_2)_2$: C, 87.23; H, 9.46; N, 2.08. Found: C, 86.48; H, 9.21; N, 1.55. IR (KBr, cm^{-1}): 2954 (s), 2926 (s), 2854 (s), 1862 (w), 1629 (w), 1603 (m), 1580 (w), 1496 (m), 1463 (s), 1378 (m), 1268 (m), 879 (m), 825 (m), 802 (s), 761 (w), 722 (w).

2.2.5.4. PFCz5R0. 3,6-dibromo-N-decylcarbazole **6** (209.4 mg, 0.45 mmol), **BrCzR0** (65.8 mg, 0.05 mmol), 2,7-bis-(trimethyleneborate)-9,9-dioctylfluorene **7** (279.2 mg, 0.5 mmol) were used in the polymerization. ^{1}H NMR (300 MHz, $CDCl_3$): δ 8.68–8.58 (m, ArH of Ir (PPQ)), 8.50 (s, 2H), 7.85 (d, J = 7.5 Hz, 4H), 7.77–7.73 (m, 4H), 7.53 (d, J = 8.4 Hz, 2H), 6.96–6.90 (m, ArH of Ir(PPQ)), 6.65–6.58 (m, ArH of Ir (PPQ)), 4.39 (s, 2H), 2.14 (br, 4H), 1.96 (br, 2H), 1.26–1.11 (m, 38H), 0.89–0.74 (m, 9H). Anal Calcd for $(C_{29}H_{40})_{50}(C_{22}H_{27}N)_{45}(C_{69}H_{61}IrN_3O_2)_5$: C, 85.86; H, 9.11; N, 2.16. Found: C, 84.95; H, 8.71; N, 2.85. IR (KBr, cm^{-1}): 2953 (s), 2926 (s), 2854 (s), 1862 (w), 1629 (w), 1603 (m), 1580 (m), 1538 (w), 1495 (m), 1463 (s), 1379 (m), 1268 (m), 879 (m), 825 (m), 802 (s), 762 (w), 723 (w).

2.2.6. General procedure of the Yamamoto polymerization

To a mixture of $Ni(COD)_2$ (0.33 g, 1.2 mmol) and 2,2′-bypyridyl (0.19 g, 1.2 mmol), 0.12 mL COD and 10 mL anhydrous DMF were added under argon. The resulting solution was kept stirring at 60 °C for 0.5 h, then slowly added to a solution of 3,6-dibromo-N-decylcarbazole **6** and 9-(iridium(III)bis(2,4-diphenyl-quinoline-N,$C^{2'}$)(quindecanedionate-12,14))-3,6-dibromocarbazole **5** with corresponding feed ratios in anhydrous DMF (2 mL). The reaction was maintained at 60 °C for 24 h in the dark. The resulting precipitate was filtered, and dissolved in DCM, then washed intensively with saturated EDTA-4Na solution. After dried with anhydrous sodium sulfate, the solution was concentrated to an appropriate volume and then poured into isopropanol to get polymer fibers. The polymer was purified by Soxhlet extraction in cyclohexane for 48 h. The reprecipitation procedure in DCM/isopropanol was then repeated for several times. The final product was obtained after drying in vacuum with a yield of 30%–50%.

2.2.6.1. PCz05R0. 3,6-dibromo-N-decylcarbazole **6** (463.0 mg, 0.995 mmol), **BrCzR0** (6.6 mg, 0.005 mmol) were used in the polymerization. ^{1}H NMR (300 MHz, $CDCl_3$): δ 8.53 (br, 2H), 7.87 (br, 2H), 7.44 (br, 2H), 4.21 (br, 2H), 1.85 (br, 2H), 1.43–1.13 (m, 14H), 0.82 (t, J = 6 Hz, 3H). Anal Calcd for $(C_{22}H_{27}N)_{99.5}(C_{69}H_{61}IrN_3O_2)_{0.5}$: C, 86.23; H, 8.84; N, 4.57. Found: C, 83.64; H, 8.64; N, 5.05. IR (KBr, cm^{-1}): 2952 (s), 2925 (s), 2853 (s), 1859 (w), 1629 (w), 1605 (m), 1473 (s), 1379 (m), 1348 (s), 1302 (m), 1268 (s), 1241 (s), 1135 (s), 874 (s), 797 (s), 722 (w).

2.2.6.2. PCz1R0. 3,6-dibromo-N-decylcarbazole **6** (460.6 mg, 0.99 mmol), **BrCzR0** (13.2 mg, 0.01 mmol) were used in the polymerization. ^{1}H NMR (300 MHz, $CDCl_3$): δ 8.51 (br, 2H), 7.85 (br, 2H), 7.41 (br, 2H), 4.19 (br, 2H), 1.84 (br, 2H), 1.42–1.11 (m, 14H), 0.82 (t, J = 6.3 Hz, 3H). Anal Calcd for $(C_{22}H_{27}N)_{99}(C_{69}H_{61}IrN_3O_2)_1$: C, 85.96; H, 8.78; N, 4.55. Found: C, 84.56; H, 9.11; N, 4.10. IR (KBr, cm^{-1}): 2952 (s), 2925 (s), 2853 (s), 1859 (w), 1629 (w), 1604 (m), 1472 (s), 1379 (m), 1347 (s), 1301 (m), 1268 (m), 1235 (s), 1136 (m), 874 (m), 797 (s), 722 (w).

2.2.6.3. PCz2R0. 3,6-dibromo-N-decylcarbazole **6** (456.0 mg, 0.98 mmol), **BrCzR0** (26.3 mg, 0.02 mmol) were used in the

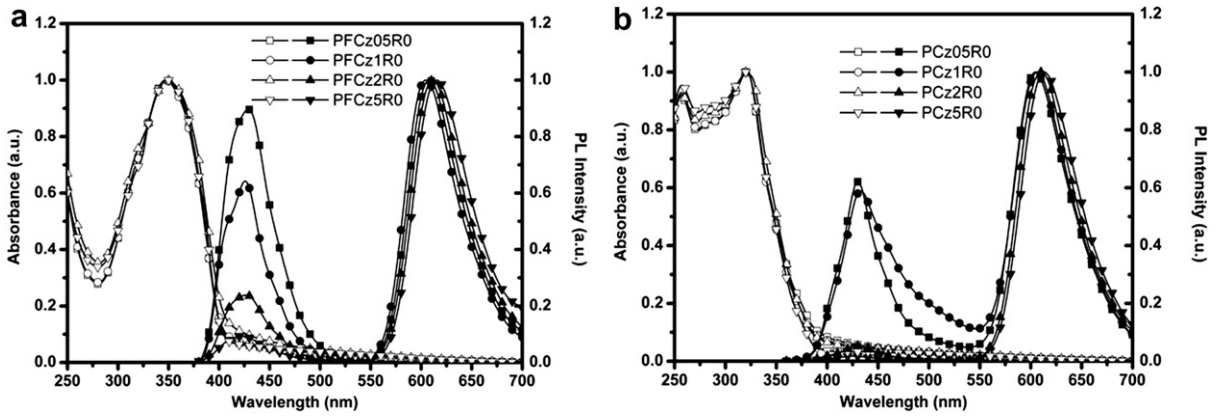

Fig. 5. The absorption and PL spectra of the polymers in films (a) PFCz-based polymers; (b) PCz-based polymers.

polymerization. ^{1}H NMR (300 MHz, $CDCl_3$): δ 8.53 (br, 2H), 7.86 (br, 2H), 7.42 (br, 2H), 6.96–6.90 (m, ArH of Ir(PPQ)), 6.61–6.58 (m, ArH of Ir(PPQ)), 4.19 (br, 2H), 1.84 (br, 2H), 1.44–1.10 (m, 14H), 0.82 (t, J = 6 Hz, 3H). Anal Calcd for $(C_{22}H_{27}N)_{98}(C_{69}H_{61}IrN_3O_2)_2$: C, 85.44; H, 8.65; N, 4.52. Found: C, 84.65; H, 8.54; N, 4.73. IR (KBr, cm^{-1}): 2952 (s), 2925 (s), 2853 (s), 1859 (w), 1629 (m), 1605 (s), 1578 (m), 1537 (w), 1471 (s), 1379 (s), 1348 (s), 1301 (s), 1268 (s), 1235 (s), 1136 (s), 874 (s), 797 (s), 722 (w).

2.2.6.4. PCz5R0. 3,6-dibromo-N-decylcarbazole **6** (442.0 mg, 0.95 mmol), **BrCzR0** (65.8 mg, 0.05 mmol) were used in the polymerization. ^{1}H NMR (300 MHz, $CDCl_3$): δ 8.52 (br, 2H), 7.85 (br, 2H), 7.44 (br, 2H), 6.96–6.91 (m, ArH of Ir(PPQ)), 6.64–6.59 (m, ArH of Ir (PPQ)), 4.21 (br, 2H), 1.84 (br, 2H), 1.44–1.11 (m, 14H), 0.82 (t, J = 6.3 Hz, 3H). Anal Calcd for $(C_{22}H_{27}N)_{95}(C_{69}H_{61}IrN_3O_2)_5$: C, 84.04; H, 8.31; N, 4.43. Found: C, 83.38; H, 8.34; N, 5.18. IR (KBr, cm^{-1}): 2952 (s), 2925 (s), 2853 (s), 1859 (w), 1629 (w), 1604 (m), 1579 (m), 1537 (w), 1473 (s), 1379 (m), 1348 (s), 1301 (m), 1268 (s), 1235 (s), 1135 (m), 874 (s), 797 (s), 722 (w).

2.3. Device fabrication

The indium-tin oxide (ITO) glass plates were cleaned in an ultrasonic solvent bath and then baked in a heating chamber at 120 °C, and treated with O_2 plasma for 25 min before use. A 50 nm thick ITO-modifying layer of poly(ethylenedioxythiophene):poly (styrene sulfonic acid) (PEDOT:PSS) was spin-coated on top of the ITO and then baked for 40 min at 120 °C. Thin films of the polymers were spin-coated from their solution in chlorobenzene (15 mg mL^{-1}). The substrate was then thermally annealed in vacuum at 100 °C for 30 min. After being cooled, the substrate was transferred to a vacuum thermal evaporator. A 10 nm thick layer of Ca was deposited at a pressure of 2×10^{-3} Pa through a mask, and another layer of 100 nm thick Al was deposited on the top as a protecting layer for Ca. The active emissive area defined by the two electrodes was 10 mm^2. The hole-only devices were fabricated with the configuration of ITO/PEDOT:PSS/polymer/Au. The EL spectra, CIE coordinates, current–voltage and brightness–voltage characteristics of the devices were measured with a Spectrascan PR650 spectrophotometer in the forward direction and a computer-controlled Keithley 2400 under ambient conditions.

3. Results and discussion

3.1. Synthesis and characterization

Scheme 1 illustrates the synthetic route of the Ir complex monomer **5** (BrCzR0). This key phosphorescent monomer **5** was obtained by reacting 3,6-dibromocarbazole with a diketone-ended alkyl chain attached to its N-position (**3**) with 2,4-diphenylquinoline (PPQ)-based Ir chloride-bridged dimer [15]. And the synthesis of the corresponding electrophosphorescent polymers is shown in Scheme 2. The polymers with PFCz as the main chain were produced by a typical palladium-catalyzed Suzuki polycondensation, and after the completion of the polymerization, the polymers were sequentially end-capped by phenylboronic acid and bromobenzene. On the other hand, a modified Yamamoto coupling method was used to prepare the polymers with PCz as the main chain, which utilized a reverse order of the addition of the nickel reagent into the monomer solution, and in this way, PCz-based polymers with high molecular weights were obtained [16]. As determined by GPC (Table 1), the M_n values are around 20,000 with polydispersity indexes (PDIs) of 2.21–2.56 and 32,000–78,000 with PDIs of 1.51–2.16 for the PFCz- and PCz-based polymers, respectively. And their thermal properties were also characterized by DSC and TGA in a nitrogen atmosphere. As collected in Table 1,

Table 2
Device Performance of the Polymers.

Polymer	λ_{max} (nm)	Voltage[a] (V)	Luminance[b] (cd/m^2)	EQE[b] (%)	LE[b] (cd/A)	PE[b] (lm/w)	CIE (x,y)
PFCz05R0	608	4.2	3968	1.5	2.3	1.1	(0.60,0.35)
PFCz1R0	608	4.2	3745	1.2	1.7	0.7	(0.62,0.36)
PFCz2R0	612	5.3	2057	0.5	0.7	0.2	(0.63,0.36)
PFCz5R0	620	5.3	638	0.3	0.3	0.2	(0.65,0.35)
PCz05R0	608	4.0	88	0.1	0.1	0.1	(0.56,0.35)
PCz1R0	612	4.0	425	0.2	0.3	0.1	(0.61,0.36)
PCz2R0	616	5.4	263	0.1	0.1	0.04	(0.63,0.35)
PCz5R0	620	6.0	33	0.04	0.04	0.02	(0.63,0.34)

[a] The voltage at a luminance of 1 cd/m^2.
[b] The maximum values for the luminance, external quantum efficiency (EQE), luminous efficiency (LE) and power efficiency (PE).

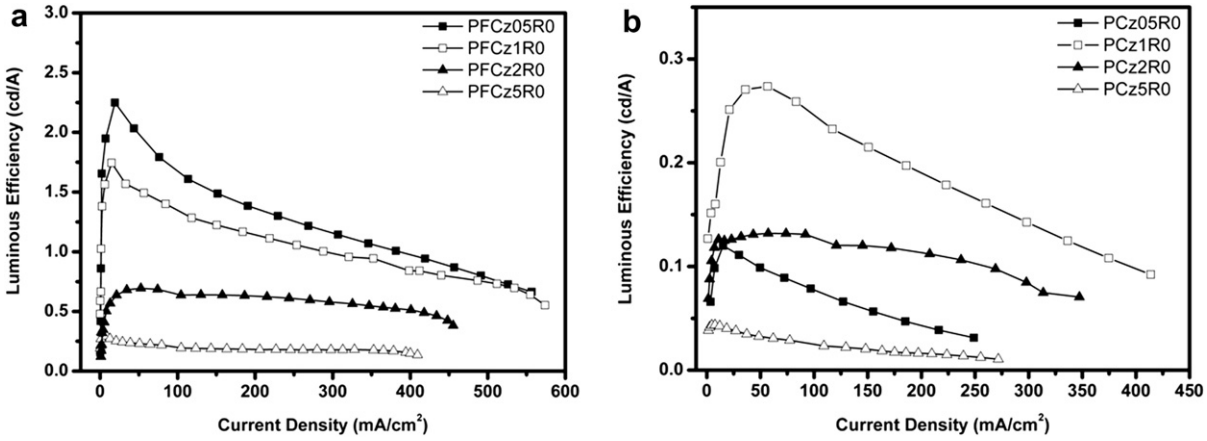

Fig. 6. The current density dependence of the luminous efficiency of the polymers. (a) PFCz-based polymers; (b) PCz-based polymers.

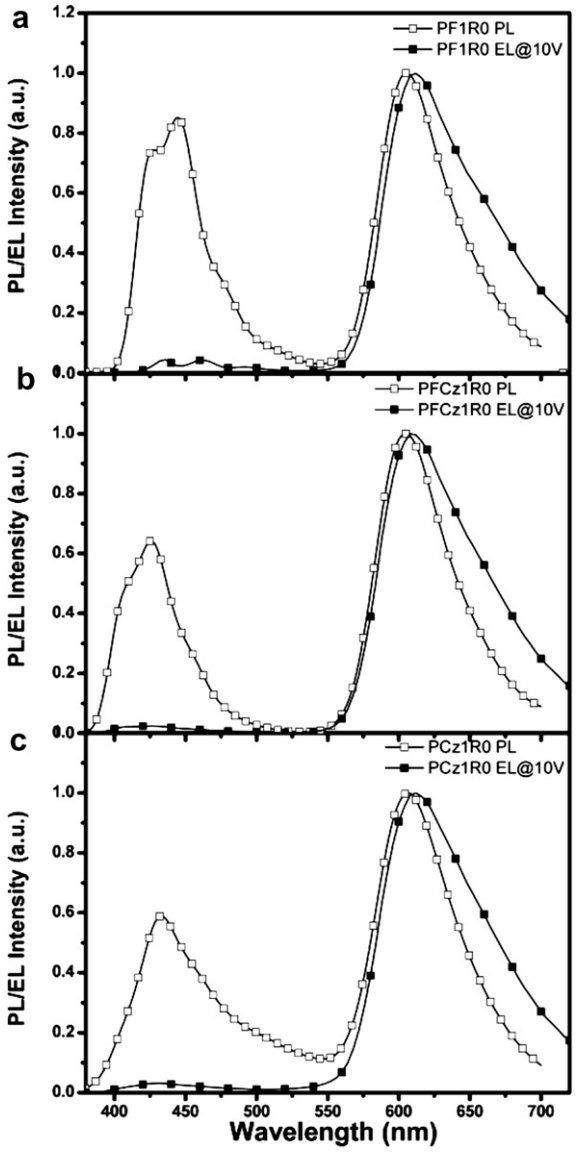

Fig. 7. The comparison of PL and EL spectra (at a driving voltage of 10 V) of PF1R0 (a), PFCz1R0 (b) and PCz1R0 (c).

the PFCz-based polymers, PFCz05R0–PFCz5R0, have similar glass transition temperatures (T_g: 101–106 °C), corresponding to that of the PFCz backbone (100 °C), due to the attachment of the low content of the Ir complex in the final polymers. Additionally, PFCz05R0–PFCz2R0 show close decomposition temperatures (T_d: 416–418 °C), indicating their good thermal stability. However, the T_d of PFCz5R0 decreases to 358 °C when higher content of $(PPQ)_2Ir(acac)$ is incorporated to the final polymers. As for the PCz-based polymers, PCz05R0- PCz5R0, the same trend was observed.

Fig. 1(a) and (b) give the IR spectra of the resulting polymers in comparison with PFCz and PCz, respectively. As can be seen clearly, the characteristic bands at 1579 and 1538 cm^{-1} assigned to the acetylacetone group of $(PPQ)_2Ir(acac)$ (R0) become more intense as the feed ratio increases, suggesting the increasing content of this Ir segment incorporated to the final polymers [17]. To quantify the actual attached number of $(PPQ)_2Ir(acac)$, ^1H NMR spectra were characterized. However, no meaningful information can be found when the feed ratio is below 2 mol %. Only when the feed ratio reaches to 2 mol %, the visible separated signals appear at 6.97–6.87 and 6.72–6.55 ppm, which can be attributed to the protons of PPQ ligand in $(PPQ)_2Ir(acac)$. Therefore, the relative ratio of the $(PPQ)_2Ir(acac)$ in the PFCz-based polymers can be calculated by comparing the integration of the ^1H NMR signals at 6.72–6.55 ppm with the sum of the first CH_2 groups of the alkyl chains to the 9-position of fluorene (δ 2.15) together with that to the

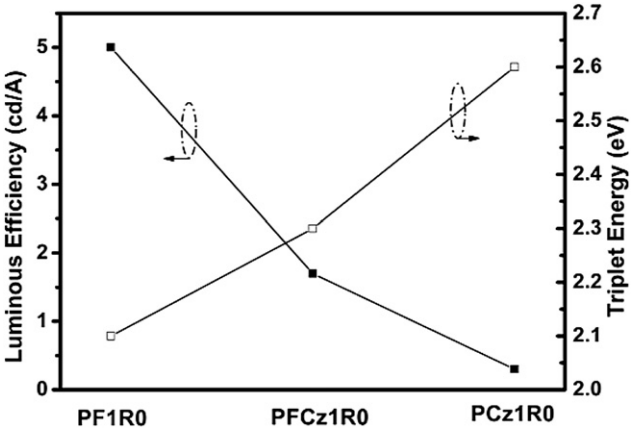

Fig. 8. The comparison of the luminous efficiency and triplet energy among PF1R0, PFCz1R0 and PCz1R0.

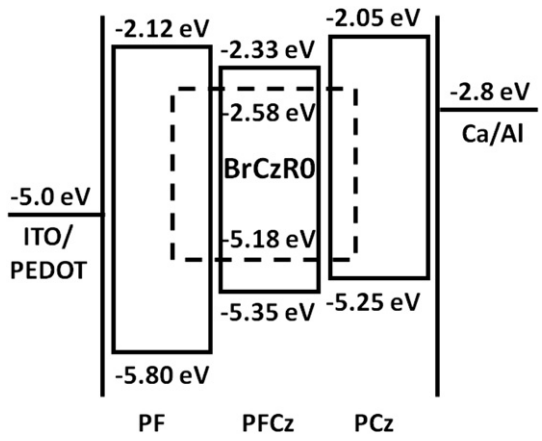

Fig. 9. The proposed energy-level diagram for the devices.

N-position of carbazole (δ 4.21). For PCz-based ones, the results are obtained in a similar way. The calculations and the feed ratios for comparison are all listed in Table 1. Similar to previously reported results, the actual Ir complex content in the final polymer is found to be substantially lower than the feed ratio of the monomer [9].

3.2. Photophysical properties

Fig. 2(a) shows UV–Vis absorption and photoluminescent (PL) spectra of the monomer BrCzR0 in solutions, and the PL spectra of PFCz and PCz in films. According to the literature [12], the absorption bands around 275 and 350 nm can be attributed to the ligand-centered (LC) transitions of the Ir complex, and the π–π^* absorptions of the carbazole moiety locate at 240 and 305 nm. The weak absorptions below 400 nm are assigned to the metal-to-ligand charge-transfer (MLCT) absorption of the Ir complex. As indicated in Fig. 2(a), the PL spectra of both PFCz and PCz have a good overlap with the MLCT absorption of the phosphorescent guest BrCzR0, which means that the Förster energy transfer from PFCz and PCz to BrCzR0 is efficient [18]. Simultaneously, in order to determine the E_T level of the polymer backbone, we measured the phosphorescent spectra of the pristine polymers at 77 K, and the results are displayed in Fig. 2(b). According to the maximum of the first vibronic mode ($S_0^{\nu=0} \leftarrow T_1^{\nu=0}$) of the corresponding phosphorescence spectra, we estimated the E_T levels of PF, PFCz and PCz to be 2.1 eV, 2.3 eV and 2.6 eV, respectively. Fig. 3 displays all energy levels of the hosts and guest. As can be clearly seen, the triplet energies of both PFCz and PCz were higher than that of BrCzR0. Compared with PF, this triplet energy enhancement would further suppress the backward energy transfer from the phosphor to the polymeric host, and avoid the loss of the triplet excitons [11,19]. To confirm our hypothesis, the transient PL spectra of PF1R0, PFCz1R0 and PCz1R0 were measured, and their lifetimes were obtained by single exponential fit of emission decay curves (Fig. 4). With the increasing triplet energy, the lifetime gradually increases from 1.15 μs of PF1R0 to 1.23 μs of PFCz1R0 and 1.46 μs of PCz1R0. This observation further demonstrates that the triplet excitons can be effectively confined on the phosphor for the electrophosphorescent polymer with higher triplet energy main chain.

Fig. 5(a) and (b) depict the UV–Vis as well as PL spectra of the PFCz- and PCz-based electrophosphorescent polymers in films, respectively. For both of these two series of polymers, the absorption spectra resemble to those of their pristine polymeric backbone, and no distinct absorptions belonging to the Ir complex are observed because of its low content loading. However, their PL spectra show obvious red light emission from the Ir complex even though the feed ratio is as low as 0.5 mol %. Moreover, the intensity of the emission from the polymer backbone decreases with the increasing feed ratio. Especially for PFCz5R0, PCz2R0 and PCz5R0, the emission from PFCz or PCz is almost quenched completely. These results indicate the efficient energy transfer from PFCz or PCz to the Ir complex. In addition, with the increasing Ir content in the final polymers, the emission shows a small red shift, which means that the aggregation exists in these polymers to some degree.

3.3. Device performance

Single layer devices with the configuration of ITO/PEDOT:PSS/Polymer/Ca/Al were fabricated and the results are summarized in Table 2. The current density dependence of luminous efficiency of the two series of polymers is displayed in Fig. 6. The best results were obtained from PFCz05R0-based device, and the maximum luminous efficiency reached to 2.3 cd/A with the Commission Internationale de L'Eclairage (CIE) coordinate of (0.60, 0.35). When the current density increased to 100 mA/cm^2, the luminous efficiency still remained as high as 1.7 cd/A, indicative of a gentle efficiency roll-off for the chemical attaching system in contrast to the physical blending system [4–6]. As for the PCz-based polymers, the device performance was relatively poor, and only 0.3 cd/A was achieved for PCz1R0.

Fig. 7 gives the PL and electroluminescence (EL) spectra of PF1R0, PFCz1R0 and PCz1R0. Similar to PF1R0, the EL spectra of PFCz1R0 and PCz1R0 are obviously different from their PL counterparts. In the EL spectra, the emission is mainly from the Ir complex guest, and the emission derived from the polymeric host is completely quenched, which demonstrates that direct charge trapping on the Ir complex is the main mechanism in the EL process [20]. However, it is interesting to note that the efficiency of PFCz1R0 and PCz1R0 is much lower than that of PF1R0 (Fig. 8), although their triplet energies of the main chain are improved. This result is out of our expectation, but we can reasonably interpret it from the standpoint of charge balance.

As can be clearly seen in Fig. 9, the HOMO levels of the polymeric backbones change at the same time while tuning the triplet energy. For example, the HOMO level increases from −5.80 eV of PF to −5.25 eV of PCz [21–23]. This improvement, on one hand, can decrease the hole injection barrier, and facilitate the efficient hole injection. On the other hand, the hole-trap depth between the

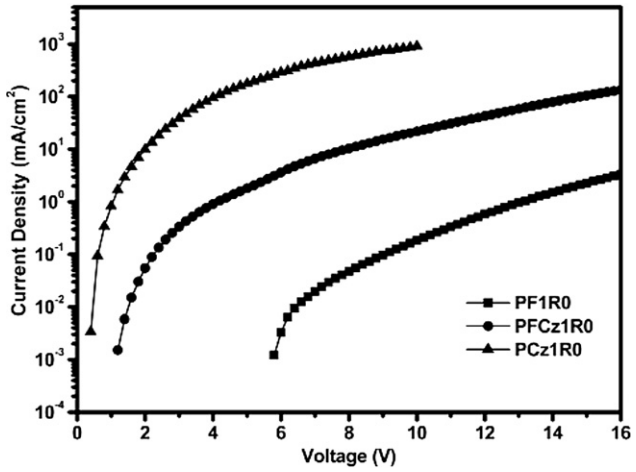

Fig. 10. Comparison of the hole current density of PF1R0, PFCz1R0 and PCz1R0.

polymeric host and the Ir guest has decreased from 0.62 eV for PF to 0.07 eV for PCz, which will weaken the hole-trap capability and enhance the hole transportation in contrary. Taking these two factors into account, the consequence is that the hole current will increase, and result in the charge imbalance in the emitting layer accompanied by the poor device performance. This can be further verified by the comparison of the hole current measured from the hole-only devices. Ongoing from PF1R0 to PFCz1R0 and PCz1R0, the hole current is found to increase in turn, as shown in Fig. 10. Consequently, the calculated hole mobility using space-charge-limited current (SCLC) method [24] improves from 1.9×10^{-12} cm^2/(Vs) of PF1R0 to 1.9×10^{-8} and 9.2×10^{-6} cm^2/(Vs) of PFCz1R0 and PCz1R0, respectively.

Based on the above-mentioned observations, we can speculate that the triplet energy of the polymeric host is not the only factor that affects the device performance of the PhPLEDs. As for the red light-emitting electrophosphorescent polymers, where the main chain has the comparable triplet energy with the Ir complex dopant, charge balance in the emissive layer plays a paramount role in determining the performance of the resulting materials.

4. Conclusions

We have synthesized red light-emitting electrophosphorescent polymers with PFCz and PCz as the main chain. Compared with PF, the triplet energy of the backbone among these polymers is improved, and the triplet excitons can be effectively confined on the Ir complex. However, the higher triplet energy of the polymer main chain doesn't mean higher luminous efficiency of the corresponding polymers. As for PFCz1R0 and PCz1R0, the maximum luminous efficiencies are 1.7 and 0.3 cd/A, respectively, which are substantially lower than that of PF1R0 (5.0 cd/A). Based on the comparison of the hole current obtained from the hole-only devices, we consider that, while tuning the triplet energy of the polymeric host, the HOMO level alters simultaneously, which leads to charge imbalance in the emitting layer, and thus poor device performance. It is believed that, from these results, charge balance must be firstly considered to develop high efficiency red light-emitting electrophosphorescent polymers.

Acknowledgements

The authors are grateful to the National Natural Science Foundation of China (No. 20923003), Science Fund for Creative Research Groups (No. 20921061), and 973 Project (2009CB623601) for financial support of this research.

References

[1] Kraft A, Grimsdale AC, Holmes AB. Angew Chem Int Ed Engl 1998;37:402–28.
[2] Baldo MA, O'Brien DF, You Y, Shoustikov A, Sibley S, Thompson ME, et al. Nature 1998;395:151–4.
[3] Baldo MA, Adachi C, Forrest SR. Phys Rev B 2000;62:10967–77.
[4] Lee CL, Lee KB, Kim JJ. Appl Phys Lett 2000;77:2280–2.
[5] Noh YY, Lee CL, Kim JJ, Yase K. J Chem Phys 2003;118:2853–64.
[6] Gong X, Ostrowski JC, Bazan GC, Moses D, Heeger AJ, Liu MS, et al. Adv Mater 2003;15:45–9.
[7] Chen X-W, Liao J-L, Liang Y-M, Ahmed MO, Tseng H-E, Chen S-A. J Am Chem Soc 2003;125:636–7.
[8] Jiang JX, Jiang CY, Yang W, Zhen HG, Huang F, Cao Y. Macromolecules 2005; 38:4072–80.
[9] Ma ZH, Ding JQ, Zhang BH, Mei CY, Cheng YX, Xie ZY, et al. Adv Funct Mater 2010;20:138–46.
[10] Ding JQ, Lv JH, Cheng YX, Xie ZY, Wang LX, Jing XB, et al. Adv Funct Mater 2008;18:2754–62.
[11] Sudhakar M, Djurovich PI, Hogen-Esch TE, Thompson ME. J Am Chem Soc 2003;125:7796–7.
[12] Ding JQ, Gao J, Fu Q, Cheng YX, Ma DG, Wang LX. Synth Met 2005;155: 539–48.
[13] You Y, Kim SH, Jung HK, Park SY. Macromolecules 2006;39:349–56.
[14] Evans NR, Devi LS, Mak CSK, Watkins SE, Pascu SI, Kohler A, et al. J Am Chem Soc 2006;128:6647–56.
[15] Nonoyama M. Bull Chem Soc Jpn 1974;47:767–8.
[16] Zhang Z-B, Fujiki M, Tang H-Z, Motonaga M, Torimitsu K. Macromolecules 2002;35:1988–90.
[17] Mei CY, Ding JQ, Yao B, Cheng YX, Xie ZY, Geng YH, et al. J Polym Sci Part A: Polym Chem 2007;45:1746–57.
[18] Förster T. Discuss Faraday Soc; 1959:7–17.
[19] Cleave V, Yahioglu G, Le Barny P, Hwang DH, Holmes AB, Friend RH, et al. Adv Mater 2001;13:44–7.
[20] Gong X, Ostrowski JC, Moses D, Bazan GC, Heeger AJ. Adv Funct Mater 2003; 13:439–44.
[21] Yuan M-C, Shih P-I, Chien C-H, Shu C-F. J Polym Sci Part A: Polym Chem 2007; 45:2925–37.
[22] Li YN, Ding JF, Day M, Tao Y, Lu JP, D'Iorio M. Chem Mater 2004;16:2165–73.
[23] Huang J, Niu YH, Yang W, Mo YQ, Yuan M, Cao Y. Macromolecules 2002;35: 6080–2.
[24] Chu TY, Song OK. Appl Phys Lett 2007;90:203512–4.